

Symmetry mediated tunable molecular magnetism on a 2D material

Yuqi Wang^{1,2*}, Soroush Arabi^{1,2,3}, Klaus Kern^{1,4} & Markus Ternes^{2,3*}

¹Max Planck Institute for Solid State Research, Heisenbergstrae 1, D-70569 Stuttgart, Germany.

²Peter-Grünberg-Institute, Forschungszentrum Jülich, D-52425 Jülich, Germany.

³Institute of Physics, RWTH Aachen University, D-52074 Aachen, Germany.

⁴Institut de Physique, École Polytechnique Fédérale de Lausanne, CH-1015 Lausanne, Switzerland.

*corresponding authors: yuqi.wang@fkf.mpg.de; ternes@physik.rwth-aachen.de

The induction of unconventional superconductivity by twisting two layers of graphene a small angle was groundbreaking¹, and since then has attracted widespread attention to novel phenomena caused by lattice or angle mismatch between two-dimensional (2D) materials². While many studies address the influence of angle mismatch between layered 2D materials^{2,3,4}, the impact of the absorption alignment on the physical properties of planar molecules on 2D substrates has not been studied in detail. Using scanning probe microscopy (SPM) we show that individual cobalt phthalocyanine (CoPc) molecules adsorbed on the layered superconductor 2H-NbSe₂ change drastically their charge and spin state when the symmetry axes of the molecule and the substrate are twisted with respect to each other. The CoPc changes from an effective spin-1/2 as found in gas-phase⁶ to a molecule with non-magnetic ground-state. On the latter we observe a singlet-triplet transition originating from an antiferromagnetic

interaction between the central-ion spin and a distributed magnetic moment on the molecular ligands. Because the Ising superconductor 2H-NbSe₂ lacks inversion symmetry and has large spin-orbit coupling⁷ this intramolecular magnetic exchange has significant non-collinear DzyaloshinskiiMoriya (DM)^{8,9} contribution.

Symmetry as a fundamental concept enables to classify properties of molecules and materials such as their optical activity, electronic bandstructure, or vibration modes¹⁰. The molecular symmetry can be changed without modifying its structure by adsorbing the molecule on a sample with a dissimilar point-group. In particular, low dimensional 2D materials are potentially interesting as platforms because of their intrinsic slowly decaying long-range interactions and the resulting extended coherence¹¹. Especially the surface of H phase transition metal dichalcogenides (TMDs) provide broken in-plane inversion symmetry and significant spin-orbit coupling induced by the central 4*d* metal ions. These properties together are key for introducing non-collinear magnetism via antisymmetric DM exchange interactions in adsorbed magnetic systems¹².

We choose CoPc, a highly symmetric metal-organic complex with flat adsorption geometry, on superconducting 2H-NbSe₂ to explore the influence of symmetry on the magnetic properties of metal-organic molecules by means of SPM. We find two stable adsorption sites of the molecules (Fig. 1a, c) which differ in their in-plane orientation: The molecule is either aligned or twisted by 15° with respect to the main surface directions (Fig. 1d, f). Constant-height SPM images also show slight differences in the topographic appearance of the two types hinting to a distinction between their electronic structures. At first glance both types of CoPc molecules have retained their cross-

like appearance, however, a closer inspection reveals that the topography of the molecules has only mirror symmetry.

We can rationalize the observation of the two differently adsorbed CoPc molecules by noticing that the difference between C_{3v} symmetry of the surface and C_{4v} symmetry of the molecules completely breaks all nontrivial rotational symmetries leaving the mirror symmetries the only retaining ones of the system (for details see SOM). Therefore, to reach maximum symmetry, one of the three σ_v mirror planes of the sample can be either aligned to one of the two σ_v or the two σ_d mirror planes of the CoPc molecules, resulting naturally in the two different adsorption geometries with 15° rotational difference. Those molecules in which the σ_v of the sample is aligned with their σ_d have magnetic properties similar to CoPc in the gas phase with an effective spin $S = 1/2$ that originates from an unpaired electron at the central Co^{2+} ion¹³. We label these molecules CoPc_d. Contrarily, molecules in which the σ_v of the sample and of the molecule are aligned couple stronger to the substrate and enable charge transfer between the molecular orbitals and the sample. We label these molecules as CoPc_v.

We now characterize in detail the magnetic state of CoPc_d by dI/dV spectroscopy using a Pb-coated SC tip with an effective gap of $\Delta_T \approx 1.15$ meV (for details see methods). Placing the tip of our SPM over the bare sample we observe a gap of $\pm(\Delta_S + \Delta_T)$ due to SC – SC tunneling between tip and sample ($\Delta_S \approx 1.3$ meV) while we measure a pair of peaks at $\approx \pm 1.8$ meV on the molecule (Fig. 2a, b). These peaks originate from the scattering of Cooper pairs at the unscreened magnetic moment of the CoPc_d molecule leading to a pair of Yu-Shiba-Rusinov (YSR) states

within the SC gap of the surface¹⁴⁻¹⁷. We find good agreement with the measured data when simulating these YSR states using a scattering model in which the impurity is treated in classical approximation with an effective magnetic moment of $\frac{1}{2}\pi\rho_S J_S S = -0.60 \pm 0.02$ and where J_S is the coupling strength between the Co^{2+} ion and the sample, ρ_S is the density of electron states of the sample in the normal conducting phase, and S is the effective spin of the central ion (for details see SOM)¹⁸. The asymmetric intensity between the peaks at positive and negative bias indicates that particle-hole symmetry is broken which we account for by an additional Coulomb scattering of $\pi\rho_S U = 0.28 \pm 0.02$.

In order to infer the spin of the CoPc_d , we apply a magnetic field $B \geq 5$ T perpendicular to the sample surface that is strong enough to suppress SC in tip and sample. Contrarily to the $B = 0$ data, we now observe split peaks around zero bias (Fig. 2c), typical for an $S = 1/2$ spin in the weak coupling Kondo regime where the Zeeman energy $E_Z = g\mu_B B$ is larger than the Kondo energy $k_B T_K$ (μ_B is the Bohr magneton and k_B is the Boltzmann constant)¹⁹. The Kondo temperature T_K is the characteristic temperature below which magnetic exchange interactions between the doublet state and the conduction electrons of the sample screen the local magnetic moment of the molecule forming a many-electron singlet state^{20,21}. A linear regression of the peak splitting leads to a Landé g -factor of 1.54 ± 0.02 , significantly smaller than the one for a free electron (Fig. 2d). The interception of the fit with the abscissa is not at the origin but at a $B_K = 0.67 \pm 0.19$ T. In linear approximation, B_K is the minimal field strength necessary for splitting the Kondo singlet state and enables the estimation of $T_K \approx g\mu_B B_K / k_B = 0.77 \pm 0.24$ K²². Because the Kondo screening energy is much smaller than the Cooper pair binding energy of the sample, i. e. $\Delta_S \gg k_B T_K$, the

opening of the SC gap at $B = 0$ hinders Kondo screening by depleting the available electronic states at the Fermi energy, in perfect agreement with the appearance of the YSR-states²³.

We now turn our interest towards the CoPc_v molecules. On these molecules we detect strong spectroscopic features at $|V| \approx 23 - 25$ mV, but neither a Kondo peak close to zero bias nor YSR states inside the SC gap (Fig. 3a, b). Indeed, comparing the SC gap measured on the bare surface and on the molecule reveal no detectable difference at $B = 0$ (Fig. 3b). In contrast to the observation on CoPc_d, even at B -fields large enough to suppress SC, we observe only a flat and featureless spectrum suggesting that CoPc_v is not $S = 1/2$, but has a non-magnetic ground-state (Fig. 3b). However, our observation of a strong conductance increase at higher absolute biases is a clear indicator for inelastic excitations²¹. At $B = 0$ the dI/dV spectrum shows sharp peaks on top of the steps which are induced by the convolution with the SC tip and sample spectrum²⁴. This convolution also leads to an apparent shift of the excitation energy by $\Delta_T + \Delta_S$. By increasing the B -field we observe that the dI/dV steps or, equivalently, the peaks in d^2I/dV^2 successively split (Fig. 3c–f), proving that the feature is of magnetic origin. Note, our observations are not compatible with vibrational excitations which have been observed on CoPc molecules adsorbed on Ag(110) at similar energy but with much lower intensity²⁵.

Kelvin-Probe measurements on top of the Co²⁺ ion show only a negligible change of the local work function, but a stronger hybridization between the CoPc_v molecule and sample (see SOM). This suggests that the change of symmetries by the slight change of orientation is accompanied by a charge transfer between the ligands of the CoPc_v molecule and the substrate. This transfer

induces an additional magnetic moment which interacts antiferromagnetically with the moment at the central metal ion leading to the observed singlet ground state of CoPc_v. However, Heisenberg-like interactions between the two spins alone would lead to a triplet of excitations at high enough B -fields (Fig. 3g). In contrast, we observe a splitting in only two distinguishable excitations. Remarkably, the excitations at lower absolute energy have about twice the intensity of the ones at higher absolute energy. This points to additional non-collinear interactions between both spins. To get a deeper understanding we model the excitation energy using the following Hamiltonian:

$$\hat{H}_{\text{CoPc}_v} = \sum_{i=1,2} g\mu_B \hat{S}_z^i B + J_{ST} \cdot \hat{\mathbf{S}}_1 \cdot \hat{\mathbf{S}}_2 + \vec{D}_{ST} \cdot (\hat{\mathbf{S}}_1 \times \hat{\mathbf{S}}_2). \quad (1)$$

Here, the first term accounts for the Zeeman energy with the B -field applied perpendicular to the surface in z -direction. The second and third terms account for the interaction between the two intramolecular spins $\hat{\mathbf{S}}_i = (\frac{1}{2}\hat{\sigma}_x^i, \frac{1}{2}\hat{\sigma}_y^i, \frac{1}{2}\hat{\sigma}_z^i)$ ($\sigma_{x,y,z}$ are the standard Pauli matrices) by an isotropic Heisenberg coupling term J_{ST} and the non-collinear Dzyaloshinskii-Moriya (DM)^{8,9} interaction vector \vec{D}_{ST} . We find an excellent agreement between our measured data and simulations which employs equation 1 and a perturbative tunneling model²¹ using a Heisenberg interaction strength of $J_{ST} = 21.6 \pm 0.5$ meV and a DM interaction vector \vec{D}_{ST} which lies in the surface plane and has a strength of $|\vec{D}_{ST}| = (0.45 \pm 0.1) \times J_{ST}$ (Fig. 3d, f). The apparent visibility of only two transitions originates from an asymmetric shift of the triplet state energies so that even at high B -fields two of them can not be separated and overlay in the observed dI/dV spectra (Fig. 3h, i). This also clearly exclude that \vec{D}_{ST} has a significant out-of-plane component.

In contrast to the intermolecular interaction found in layers of CoPc²⁶, here the main interaction between both spins on the CoPc_v molecule is mediated by intramolecular superexchange and

varies only slightly ($\pm 2.5\%$) with adsorption position on the charge-density-wave modulated 2H-NbSe₂ surface (see SOM). However, the significant DM coupling can not originate from within the flat molecule. Presumably it is due to interactions between the magnetic moments in the CoPc and the Nb *d*-orbitals of the 2H-NbSe₂^{27,28} resulting in an in-plane DM vector (Fig. 4a)²⁹, in agreement with the experimental data.

To study the excitation of CoPc_v in greater detail we take spectra on a grid of points covering one CoPc_v molecule. At every point we determine J_{ST} assuming a constant ratio $|\vec{D}_{ST}|/J_{ST} = 0.45$ and the intensity of the inelastic conductance relative to the total conductance, $A = \sigma_{\text{inel.}}/(\sigma_{\text{el.}} + \sigma_{\text{inel.}})$ (Fig. 4b,c). The J_{ST} map clearly reflects the 4-fold symmetry of the bare molecule (Fig. 4b). The observed small variations of J_{ST} with tip position are due to attractive mechanical forces exerted by the tip which bend the molecule and changes thereby the intramolecular magnetic coupling (see SOM).

In stark contrast to the J_{ST} map, the A -map shows clear mirror symmetry along the σ_v axes of molecule and surface, and a strong variation over the molecule with A ranging from $\approx 0.5-0.9$. This map describes the spatial distribution of the spin excitation intensity, which is correlated to the relative local density of states of the orbitals containing the unpaired spins³⁰. Surprisingly, we detect large A not only on the central Co²⁺ ion but also on the phthalocyanine ring as two, c-shaped lobes symmetrically around the mirror plane, clearly marking this direction as the one in which \vec{D}_{ST} lies. While part of the detailed sub-structure also depends on the tip apex, we note the faint lines of increased A which link the central Co²⁺ ion via the N-atoms to the benzene rings of the

molecule.

To conclude, we have revealed the key role of symmetries between substrate and adsorbate for the spin state and the intramolecular interactions of CoPc molecules on 2H-NbSe₂. While CoPc_d has an unpaired electron in the d_{z^2} -orbital of the central Co²⁺ ion¹³ which couples to the sample leading either to YSR states or to Kondo screening, the two electron spins in CoPc_v couple antiferromagnetically. The reduced symmetry and the strong spin-orbit coupling of the 2H-NbSe₂ surface induce significant non-collinear DM coupling in CoPc_v which lead to an unbalanced field splitting of the singlet-triplet excitation.

Our work demonstrates that the spin state of adsorbed molecules can strongly depend on subtle variations of the twist angle with respect to the substrate which opens a new path for controlling and engineering more complex spin structures. Additionally, the substrate mediated non-collinear interaction in metal-organic molecules is a promising platform for exploiting phenomena such as one-dimensional spin spirals³¹ or topological superconductivity.

Methods

Experimental procedure. The 2H-NbSe₂ single crystal was cleaved by attaching an adhesive Kapton polyimide tape to the crystal surface and pulling it off at a base pressure of $p \leq 10^{-8}$ mbar. CoPc molecules were then deposited from a Knudsen cell evaporator held at 410°C onto the freshly cleaved 2H-NbSe₂ at room temperature and $p \leq 10^{-9}$ mbar. The SPM experiments were performed using a home-built combined scanning tunneling and atomic force microscope operating

in ultrahigh vacuum ($p \leq 10^{-10}$ mbar), at fields perpendicular to the sample surface of up to 14 T, and at a base temperature of 1.2 K. The differential conductance (dI/dV) spectra were detected by modulating the bias voltage V with a sinusoidal of 0.05 – 0.2 mV amplitude and 617 Hz frequency utilizing a lock-in amplifier. We functionalized the bare Pt tip by indenting it into a Pb surface by several hundreds of nm repeatedly until it showed a bulk-like superconducting gap. The tip is mounted on a quartz tuning fork with a resonance frequency of $f_0 = 29,067$ Hz, a stiffness of $k = 1800$ N/m, and a Q -factor of $\approx 60,000$. Tuning fork oscillation amplitudes of 50 pm were used to measure the forces acting between tip and sample by detecting the frequency shift df of the tuning fork.

References

1. Cao, Y. *et al.* Unconventional superconductivity in magic-angle graphene superlattices. *Nature* **556**, 43–50 (2018).
2. Cao, Y. *et al.* Correlated insulator behaviour at half-filling in magic-angle graphene superlattices. *Nature* **556**, 80 (2018).
3. Sharpe, A. L. *et al.* Emergent ferromagnetism near three-quarters filling in twisted bilayer graphene. *Science* **365**, 605–608 (2019).
4. Chen, G. *et al.* Evidence of a gate-tunable Mott insulator in a trilayer graphene moiré superlattice. *Nat. Phys.* **15**, 237–241 (2019).

5. Chen, G. *et al.* Signatures of tunable superconductivity in a trilayer graphene moiré superlattice. *Nature* **572**, 215–219 (2019).
6. Mugarza, A. *et al.* Electronic and magnetic properties of molecule-metal interfaces: Transition-metal phthalocyanines adsorbed on Ag(100). *Phys. Rev. B* **85**, 155437 (2012).
7. Xi, X. *et al.* Ising pairing in superconducting NbSe₂ atomic layers. *Nat. Phys.* **12**, 139–143 (2016).
8. Dzialoshinskii, I. Thermodynamic theory of weak ferromagnetism in antiferromagnetic substances. *Sov. Phys. JETP* **5**, 1259–1272 (1957).
9. Moriya, T. Anisotropic superexchange interaction and weak ferromagnetism. *Phys. Rev.* **120**, 91 (1960).
10. Cotton, F. A. *Chemical applications of group theory* (John Wiley & Sons, 2003).
11. Ménard, G. C. *et al.* Coherent long-range magnetic bound states in a superconductor. *Nat. Phys.* **11**, 1013–1016 (2015).
12. Bode, M. *et al.* Chiral magnetic order at surfaces driven by inversion asymmetry. *Nature* **447**, 190–193 (2007).
13. Kezilebieke, S., Dvorak, M., Ojanen, T. & Liljeroth, P. Coupled Yu-Shiba-Rusinov states in molecular dimers on NbSe₂. *Nano Lett.* **18**, 2311–2315 (2018).
14. Yu, L. Bound state in superconductors with paramagnetic impurities. *Acta Phys. Sin.* **21**, 75–91 (1965).

15. Shiba, H. Classical spins in superconductors. *Prog. Theor. Exp. Phys.* **40**, 435–451 (1968).
16. Rusinov, A. Theory of gapless superconductivity in alloys containing paramagnetic impurities. *JETP Lett.* **29**, 1101–1106 (1969).
17. Heinrich, B. W., Pascual, J. I. & Franke, K. J. Single magnetic adsorbates on s-wave superconductors. *Prog. Surf. Sci.* **93**, 1–19 (2018).
18. Salkola, M., Balatsky, A. & Schrieffer, J. Spectral properties of quasiparticle excitations induced by magnetic moments in superconductors. *Phys. Rev. B* **55**, 12648 (1997).
19. Zhang, Y. *et al.* Temperature and magnetic field dependence of a Kondo system in the weak coupling regime. *Nat. Commun.* **4**, 2110 (2013).
20. Kondo, J. Effect of ordinary scattering on exchange scattering from magnetic impurity in metals. *Phys. Rev.* **169**, 437 (1968).
21. Ternes, M. Probing magnetic excitations and correlations in single and coupled spin systems with scanning tunneling spectroscopy. *Prog. Surf. Sci.* **92**, 83–115 (2017).
22. Žitko, R., Peters, R. & Pruschke, T. Splitting of the Kondo resonance in anisotropic magnetic impurities on surfaces. *New J. Phys.* **11**, 053003 (2009).
23. Franke, K., Schulze, G. & Pascual, J. Competition of superconducting phenomena and Kondo screening at the nanoscale. *Science* **332**, 940–944 (2011).
24. Heinrich, B., Braun, L., Pascual, J. & Franke, K. Protection of excited spin states by a superconducting energy gap. *Nat. Phys.* **9**, 765–768 (2013).

25. Chiang, C.-l., Xu, C., Han, Z. & Ho, W. Real-space imaging of molecular structure and chemical bonding by single-molecule inelastic tunneling probe. *Science* **344**, 885–888 (2014).
26. Chen, X. *et al.* Probing superexchange interaction in molecular magnets by spin-flip spectroscopy and microscopy. *Phys. Rev. Lett.* **101**, 197208 (2008).
27. Rossnagel, K. *et al.* Fermi surface of 2H-NbSe₂ and its implications on the charge-density-wave mechanism. *Phys. Rev. B* **64**, 235119 (2001).
28. Straub, T. *et al.* Charge-density-wave mechanism in 2H-NbSe₂: Photoemission results. *Phys. Rev. Lett.* **82**, 4504 (1999).
29. Khajetoorians, A. *et al.* Tailoring the chiral magnetic interaction between two individual atoms. *Nat. Commun.* **7**, 1–8 (2016).
30. Mishra, S. *et al.* Topological frustration induces unconventional magnetism in a nanographene. *Nat. Nanotechnol.* **15**, 22–28 (2020).
31. Menzel, M. *et al.* Information transfer by vector spin chirality in finite magnetic chains. *Phys. Rev. Lett.* **108**, 197204 (2012).

Acknowledgements We thank Christian Ast, Haonan Huang, Shawulienu Kezilebieke, Peter Liljeroth, Samir Lounis, Ana Montero, and Lihui Zhou for fruitful discussions. Y. W. acknowledges support from the Alexander von Humboldt Foundation and M. T. by the Heisenberg Program (Grant No. TE 833/2-1) of the German Research Foundation.

Author contributions M. T. conceived the experiment. Y. W. and S. A. performed the SPM measurements. Y. W. and M. T. analysed and fitted the data. M. T. and K. K. supervised the project. All authors discussed the results and contributed to the manuscript.

Competing financial interests The authors declare no competing financial interests.

Data availability The relevant spectroscopic data sets used in this publication are available from the authors.

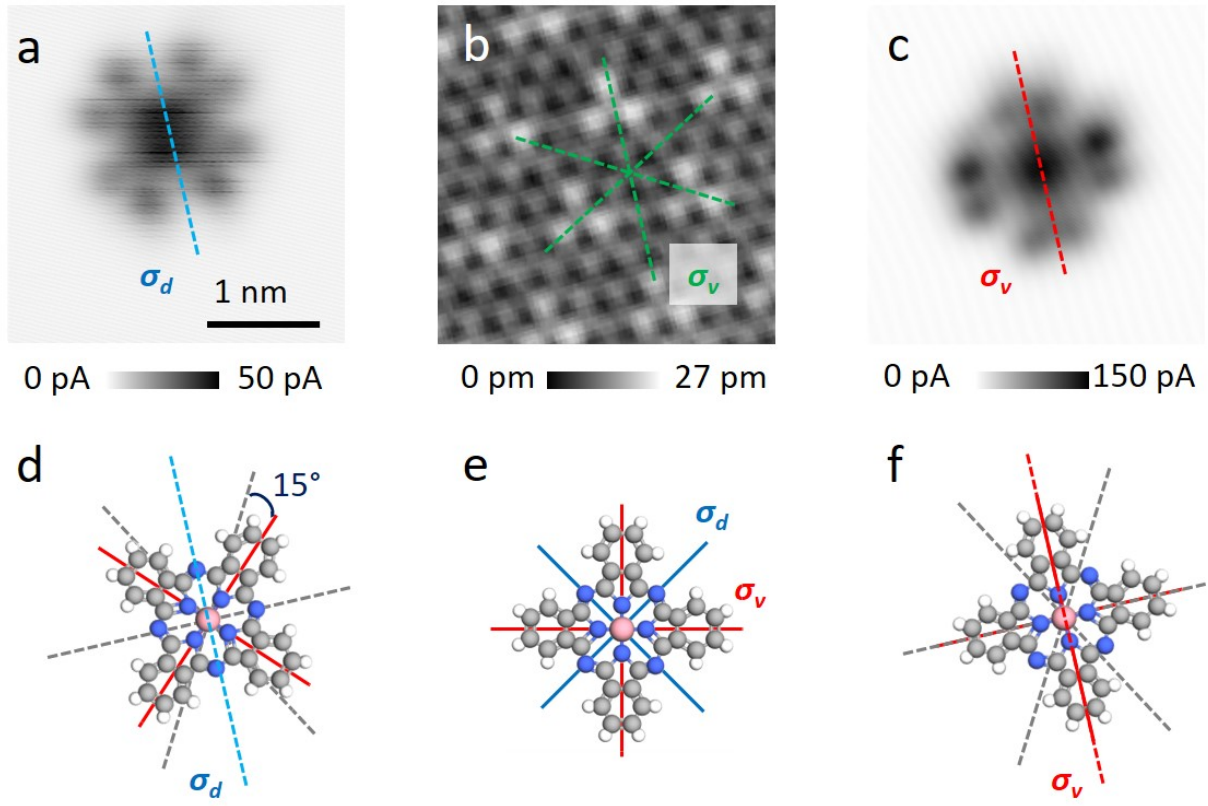


Figure 1: **Absorption symmetry and spectral fingerprint of CoPc molecules on 2H-NbSe₂.**

a, c, Constant height SPM images of two CoPc molecules ($V = 400$ mV) adsorbed in different orientations. **b**, Constant current image of the 2H-NbSe₂ surface showing the 3×3 charge density wave superstructure ($V = -10$ mV, $I = 1$ nA). Colored dashed lines in **a–c** mark the different mirror planes of the CoPc molecules and the 2H-NbSe₂ surface. **d, f**, Absorption models of CoPc molecules on 2H-NbSe₂. While the molecule in **(d)** is rotated by 15° with respect to one of the three principal axes of the substrate (grey dashed lines), the molecule in **(f)** is aligned. **e**, Model of the CoPc molecule with its vertical σ_v (red lines) and diagonal σ_d (blue lines) mirror plane symmetries.

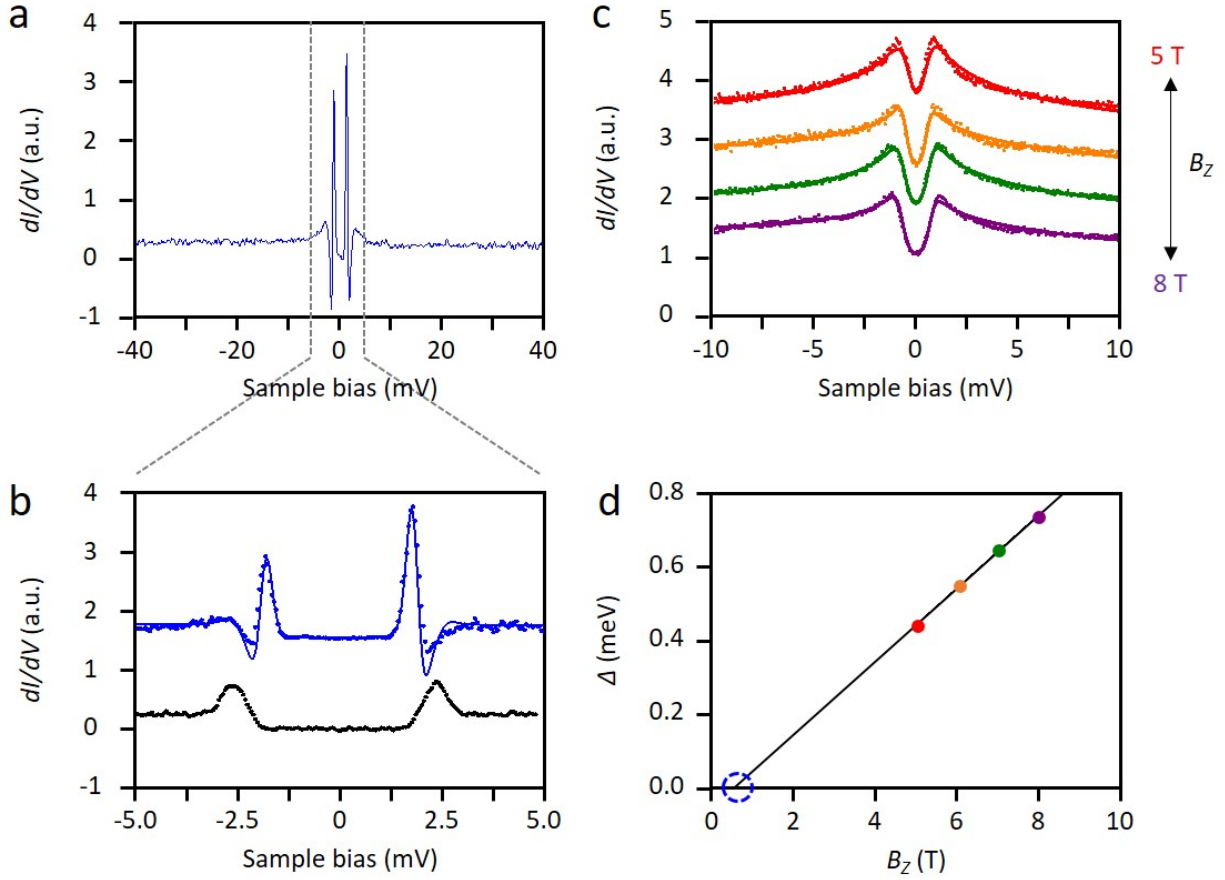


Figure 2: **Spectral features of CoPc_d**. **a, b**, Differential conductance dI/dV measured on the bare NbSe₂ sample (black dots) and the center of a CoPc_d molecule (blue dots) by using a SC tip ($V = -40$ mV, $I = 40$ pA in **(a)**; $V = -5$ mV, $I = 50$ pA in **(b)**). Full line in **(b)** is a least-square fit to a scattering model in which the magnetic impurity is treated classically. **c**, dI/dV spectra measured on CoPc_d at magnetic fields large enough to suppress SC (dotted lines, $V = -10$ mV, $I = 100$ pA) and least-square fits using a perturbative scattering model (full lines). Curves are vertically offset for clarity. **d**, Extracted splitting of the peaks in **(c)** and linear regression (full line). The dashed circle marks the crossing of the regression with the abscissa.

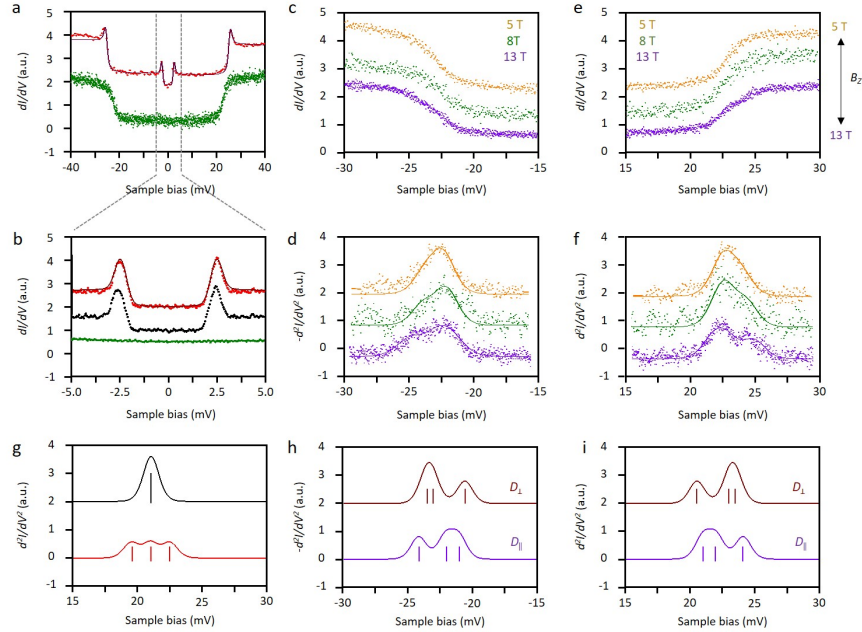


Figure 3: **The singlet – triplet transition in CoPc_v.** **a**, dI/dV spectra measured on CoPc_v at $B = 0$ (red dots) and at $B = 8$ T where SC is quenched (green dots). The full line at $B = 0$ is a least-square fit to a model which accounts for the SC gaps in tip and sample and the spin excitation. **b**, Detail of the curves in **(a)** (red and green dots) and spectrum measured on the bare NbSe₂ surface (black dots), showing that neither YSR states nor a Kondo peak can be detected on the molecule ($V = -5$ mV, $I = 50$ pA). The dark red line is a fit to a SC–SC tunneling model. **c–f**, dI/dV and numerically derived d^2I/dV^2 spectra measured on CoPc_v at $B = 5, 8$ and 13 T, respectively. Full lines in **(d,f)** are least-square fit to a perturbative transport model. The spectra reveal an asymmetric splitting of the inelastic excitation at $\approx \pm 23$ mV in field. **g**, Expected splitting of a triplet excitation at $B = 13$ T (red line) if only Heisenberg exchange interaction between both spins is taken into account. **h, i**, Accounting for an additional non-collinear DzyaloshinskiiMoriya (DM) interaction rationalized the observation if the DM vector lies in the surface plane (D_{\parallel}). A DM vector pointing out of surface (D_{\perp}) would reverse the intensity order. Curves in all panels are vertically offset for clarity.

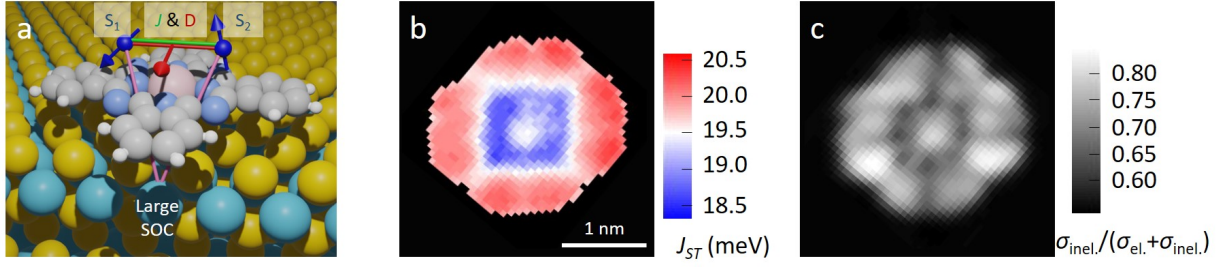


Figure 4: **Spin excitation map of CoPc_v**. **a**, Schematic ball model of the CoPc_v and its interactions. Grey, white, light blue, and pink spheres correspond to C, H, N, and Co atoms, on the molecule, respectively. Yellow and turquoise spheres correspond to Se and Nb atoms of the surface. Blue arrows indicate the two spins and the red arrow the DM vector. **b,c**, Maps of 45×45 points covering an area of $3 \times 3 \text{ nm}^2$ on which dI/dV spectra were taken and **b** the interaction strength J_{ST} and **c** the spin excitation intensity $A = \sigma_{\text{inel.}} / (\sigma_{\text{el.}} + \sigma_{\text{inel.}})$ where extracted ($V = -50 \text{ mV}$, $I = 500 \text{ pA}$). While J_{ST} map shows mainly fourfold symmetry, A -map clearly reveals the mirror plane which cuts approximately vertical through the image.